

Importance of Proton-Coupled Electron Transfer in Cathodic Regeneration of Organic Hydrides

Stefan Ilic,^{ab} Abdulaziz Alherz,^c Charles B. Musgrave^{cde} and Ksenija D. Glusac^{ab}

^a Department of Chemistry, University of Illinois at Chicago, Chicago, Illinois 60607, United States.

^b Chemical Sciences and Engineering Division, Argonne National Laboratory, Lemont, Illinois 60439, United States.

^c Department of Chemical and Biological Engineering, University of Colorado, Boulder, Colorado 80309, United States.

^d Department of Chemistry, University of Colorado, Boulder, Colorado 80309, United States.

^e Materials and Chemical Science and Technology Center, National Renewable Energy Laboratory, Golden, Colorado 80401, United States.

Table of Contents

1)	Computational Details	S2
A.	Reduction Potential (E^0) Calculations	S2
B.	Acidity (pK_a) Calculations	S2
C.	General Regeneration Pathways and Complete Table of all pK_a (in DMSO) and E^0 Data:	S4
2)	Experimental Details	S6
A.	Cyclic voltammograms of NAD^+ analogs.....	S7
B.	Cyclic voltammograms of acids	S8
C.	Cyclic voltammograms of authentic hydride samples.....	S9
E.	Protonation of A_2 -radical with HBF_4 in MeCN	S10
F.	Protonation of A_4 -radical with TfOH in MeCN	S11
G.	UV-Vis evidence for radical protonation	S11
H.	Bulk electrolyses of acridine and benzimidazole representatives	S12
I.	Electrochemical regeneration for some benzimidazole hydride with PhOH	S14
J.	Kinetic Isotope Effect for Benzimidazoles Hydride Regeneration.....	S15
3)	The $pK_a(\text{RH}^{\cdot\cdot})$ vs. $E^0_{\text{R}/\text{R}^{\cdot}}$ correlation	S15
4)	Molecular Coordinates	S16
5)	References	S30

1) Computational Details

Density functional theory calculations were performed based on the wB97XD functional¹ and the triple-zeta basis set 6-311+G(d,p)² implemented in Gaussian 16. Vibrational force constants at the wB97XD/6-311+G(d,p) level of theory were calculated to (a) validate that all geometries have only positive vibrational frequencies and (b) compute entropies, zero-point energies, and thermal corrections for the reported free energies at 298 K. Solvation effects of dimethyl sulfoxide (DMSO) were simulated using an implicit polarized continuum solvation model (CPCM).³ Hydricity values were calculated using methods developed in earlier studies.⁴

A. Reduction Potential (E^0) Calculations

Reduction potentials E^0 versus the ferrocene electrode (vs. Fc/Fc⁺) in DMSO were calculated using the wB97XD/6-311+G(d,p) level theory according to the following equation:⁵

$$\Delta G_{red} = G_{RH^-} - G_{RH^+} \quad (1)$$

$$E^0 = -27.2114 \Delta G_{red} - 5.043 \text{ V} \quad (2)$$

This was checked against experimental results and found to be in agreement within 0.2 V.

B. Acidity (pK_a) Calculations

Acidity values are essential to this work as they help determine the reaction route. pK_a values are calculated according to the following equation, following the work of Schlegel:⁶

$$pK_a = \frac{\Delta G}{2.303RT} \quad (3)$$

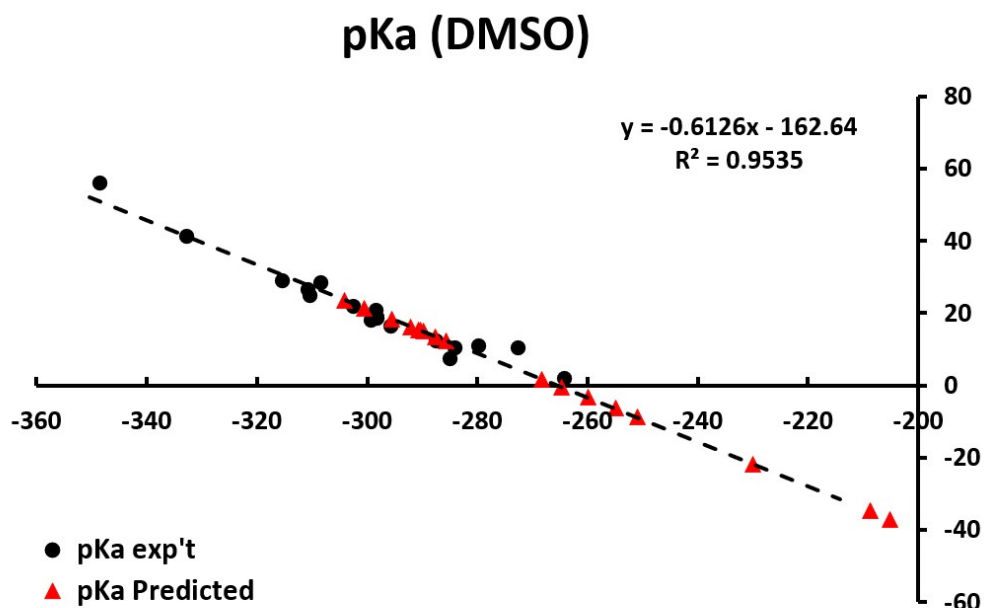
$$\Delta G = G_{A^-} - G_{AH} + G_{H^+} \quad (4)$$

In order to determine the free energy of a proton solvated in DMSO, a scaling approach is utilized where the value of G_{H^+} is averaged for a set of experimentally studied acids, presented in Table S1.

Table S1. Experimentally determined pKa values of organic acids in DMSO.⁷ The second column contains pKa values calculated using DFT calculations and using equations 3 and 4 shown above.

	pKa exp't	pKa predicted		pKa exp't	pKa predicted
benzimidazole	16.4	18.4	NH ₄ ⁺	10.5	4.3
CH ₄	56	50.8	Nicotinamide	22	22.6
HCl	1.8	-0.8	Trimethyldioxane-dione	7.4	11.9
Cyclopentadiene	18	20.6	PhCO ₂ H	11	8.7
imidazoleH	18.6	20.0	Ph ₂ NH	24.95	27.6
MeCO ₂ H	12.3	13.5	PhSH	10.3	11.4
MeOH	29	30.5	PyNH ₂	28.5	26.3
NaphthNOH	20.7	20.1	C ₅ H ₅ NNH ₂	26.5	27.7
NH ₃	41	41.2			

Plotting the DFT-calculated expression ($G_{A^-} - G_{AH}$) versus the pKa data in Table S1 yields Fig S1. The mean absolute deviation between experimentally determined and computationally predicted pKa values is 2.25 pKa units. Using the expression ($G_{H^+} = -\text{intercept}/\text{slope}$), we find that the free energy of the DMSO-solvated proton is $G_{H^+} = -265.49$ kcal/mol.



$$G_{AH} - G_{A^-}$$

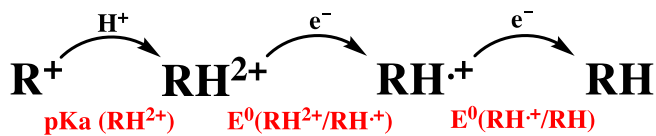
Figure S1. ($G_{A^-} - G_{AH}$) computed using wB97XD/6-311+G(d,p) level of theory versus experimentally determined pKa values reported in Table S1. Black round dots represent the experimental data set. The black dashed line is the linear regression performed on the experimental data set, with an adjusted R^2_{adj} value of 0.950. The red triangles represent pKa values of radical cation intermediates discussed in this work.

C. General Regeneration Pathways and Complete Table of all pK_a (in DMSO) and E^0 Data:

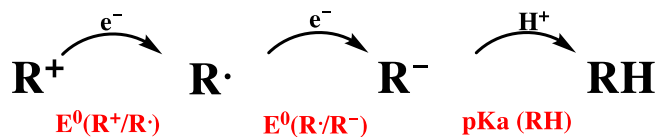
The hydride regeneration requires a net transfer of a proton and two electrons. There are three general pathways for the regeneration (Scheme S1).

Scheme S1. Three possible regeneration pathways.

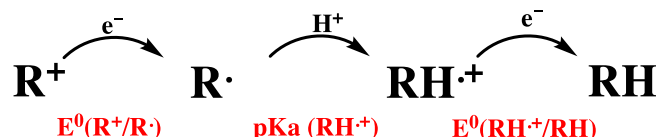
a) *proton-electron-electron (PEE)*



b) *electron-electron-proton (EEP)*



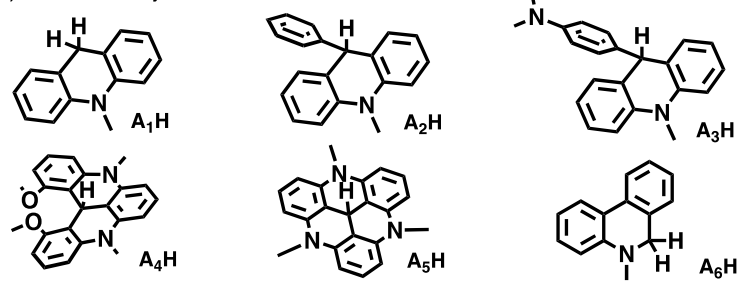
c) *electron-proton-electron (EPE)*



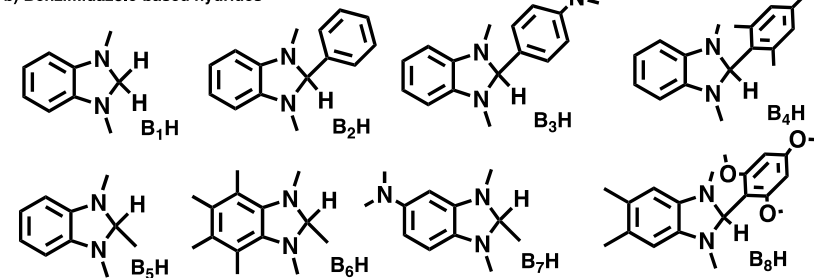
In order to investigate the possibility of each pathway, we calculated all of the relevant pK_a and E^0 values using the methods described above (Table S2). From our calculated values, it is very unlikely that the regeneration of the hydrides follows the proton-electron-electron (PEE) route because of the very negative values obtained for $pK_a(\text{RH}^{2+})$. Thus, the PEE pathway was excluded from the main manuscript.

Table S2. Structures and calculated pKa and E⁰ values for all three regeneration pathways depicted in Scheme S1.

a) Acridine-based hydrides



b) Benzimidazole-based hydrides



Molecule	pK _a			E ⁰ (V vs. Fc/Fc ⁺)				
	RH ²⁺	RH ⁺	RH	(R ⁺ /R ⁻)	(RH ²⁺ /RH ⁺)	(R ⁺ /R ⁻)	(R ⁺ /R ⁻)*	(RH ⁺ /RH)
A ₁ H	-39.4	-0.4	35.8	-1.04	1.72	-2.31	-1.83	0.25
A ₂ H	-42.1	-1.8	34.2	-1.07	1.78	-2.26	-1.79	0.28
A ₃ H	-30.6	-1.0	35.0	-1.11	0.99	-2.35	-1.86	0.20
A ₄ H	-45.8	-3.4	34.0	-1.33	1.67	-2.47	-1.95	0.18
A ₅ H	-56.5	-6.4	35.7	-1.80	1.75	-2.70	-2.15	0.28
A ₆ H	-40.1	1.7	41.0	-1.44	1.51	-2.78	-2.21	0.01
B ₁ H	-33.3	15.2	63.9	-2.57	0.87	-3.97	-3.38	-0.52
B ₂ H	-33.7	12.4	48.2	-2.30	0.96	-2.97	-2.53	-0.44
B ₃ H	-33.8	14.9	51.7	-2.59	0.86	-3.07	-2.61	-0.47
B ₄ H	-37.5	13.6	53.8	-2.70	0.91	-3.30	-2.81	-0.45
B ₅ H	-34.7	15.4	50.0	-2.66	0.88	-3.00	-2.55	-0.54
B ₆ H	-28.4	18.4	54.4	-2.79	0.52	-3.09	-2.63	-0.54
B ₇ H	-21.7	21.4	50.6	-2.83	0.22	-3.03	-2.58	-0.97
B ₈ H	-31.5	16.3	54.1	-2.69	0.69	-3.30	-2.81	-0.63

*The calculated values were scaled to experimentally obtained values due to the large mismatch, which has been observed earlier.⁴ Acridines are scaled to the values of A₂H, A₃H, A₄H and A₅H, while benzimidazoles are scaled to B₄H and B₈H.

2) Experimental Details

General Methods. All chemicals were purchased from commercial suppliers and used without further purification. 10-Methyl-9-phenylacridinium perchlorate (A_2^+) and 10-methylacridinium perchlorate (A_1^+) were purchased from TCI America. Cations ($A_6^+, {}^8A_3^+, {}^9A_4^+, {}^9A_5^+, {}^9B_1^+, {}^{10}B_2^+, {}^9B_3^+, {}^{10}B_4^+, {}^{11}B_5^+{}^{12}$ and $B_8^+{}^{13}$) and hydrides ($A_2H, {}^9A_4H, {}^9B_1H, {}^{10}B_2H, {}^9B_3H{}^{10}$ and $B_5H{}^{12}$) were synthesized according to the previously published procedures. For cyclic voltammetry (CV) measurements, the iodide salt of NAD^+ analogs was converted to perchlorate using a previously published procedure.¹⁴ Absorption spectra were measured with Ocean FX (Ocean Optics) spectrophotometer.

Choice of Solvent. DMSO was chosen as a solvent for experiments and calculations, due to good solubility of NAD^+ analogues and CO_2 , which is relevant for fuel-forming reduction catalysis. However, the high basicity of DMSO hinders the protonation of acridine-derivatives with strong acids (section 2B). Instead, these experiments were performed in acetonitrile.

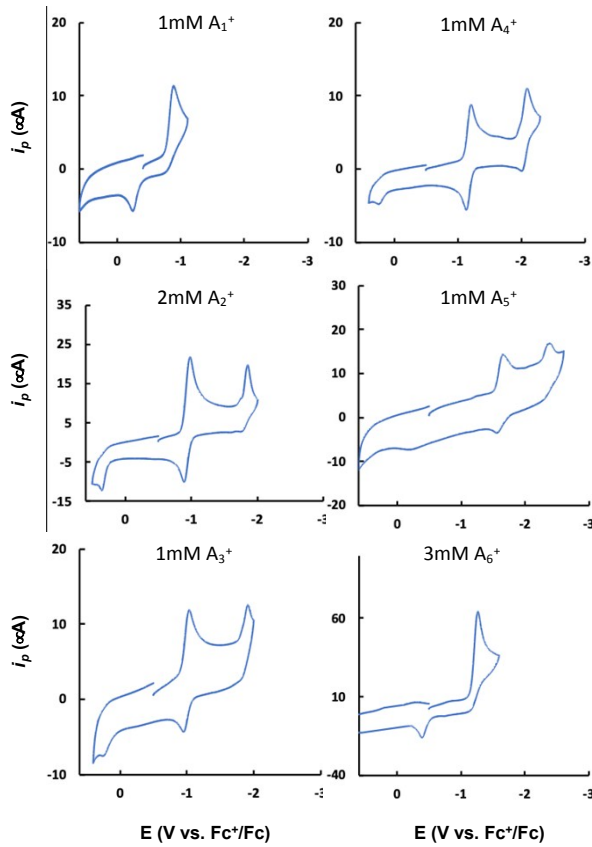
Cyclic Voltammetry. Cyclic voltammetry was performed using a BASi epsilon potentiostat in a VC-2 voltammetry cell (Bioanalytical Systems) using platinum working electrode (1.6 mm diameter, MF-2013, Bioanalytical Systems), a nonaqueous Ag/Ag^+ reference electrode (MF-2062, Bioanalytical Systems), and a platinum wire (MW-4130, Bioanalytical Systems) as a counter electrode. The spectroscopic grade solvents DMSO and MeCN and the electrolyte tetrabutylammonium perchlorate (TBAP) were purchased from Sigma-Aldrich and used as received. All cyclic voltammograms were obtained with the scan rate of 0.1 V/s. Electrochemical potentials were converted to vs. Fc/Fc^+ by adding -37 mV to the experimental potentials.¹⁵

Preparation of A_2 -radical. 50 mg of A_2^+ was dissolved in sufficient amount of deionized water (~10 mL) and 5 mL of diethyl ether was added. The solution was then purged with argon for 30 min and 20 mg of zinc was added to the mixture. The reaction was stirred for 30 min during which the deep red color was developed in the diethyl ether layer (Figure SX). The organic layer was extracted and washed with water. The prepared solution of A_2 -radical was stable over 10 days under inert atmosphere.

A. Cyclic voltammograms of NAD⁺ analogs

Fig S2 shows the electrochemical behavior for several acridine- and benzimidazole-derivatives. As mentioned in main text, unsubstituted acridines (A_1^+ and A_6^+) and benzimidazoles display irreversible reduction behavior, which results in the formation of dimers (oxidation peaks between 0 V and -1V vs. Fc/Fc⁺). The dimer oxidation peak in case of B_3^+ was confirmed with calculations ($E_{\text{dimer,ox calc}}^0 = -0.92$ V vs. Fc/Fc⁺). Acridine derivatives with stable radicals (A_2^+ , A_3^+ , A_4^+ and A_5^+) and benzimidazoles with bulky substituents (B_4^+ and B_8^+) show two well-separated reduction peaks for R⁺/R⁰ and R⁰/R⁻ conversions and formation of the hydrides (oxidation peaks between -0.5 V and 0.5 V vs. Fc/Fc⁺).

a) Acridines



b) Benzimidazoles

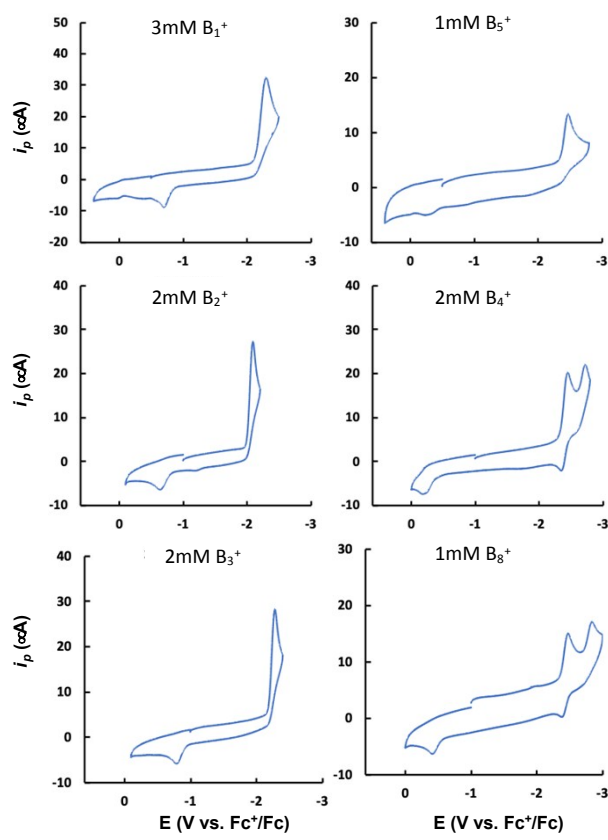


Figure S2. Cyclic voltammograms of different: a) acridines, and b) benzimidazoles.

B. Cyclic voltammograms of acids

Cyclic voltammograms represented in Fig S3 show the electrochemical behavior of acids used for regenerating acridine and benzimidazole hydrides. The growing peaks are assigned to the reduction of protons by the glassy carbon electrode and the position of the peak correlates with the acid strength. For triflic acid CV, there is a side reaction of solvent hydrolysis that might contribute to the peak profile.¹⁶

As mentioned in the main text, protonation with strong acids cannot be achieved in DMSO due to its high basicity. This is particularly evident when comparing the experiments of A_4^+ in the presence of perchloric and tetrafluoroboronic acids. In both cases, there is a peak assigned for the reduction of protons by the glassy carbon electrode (~ 1.7 V vs. Fc/Fc⁺). Since the use of acid of different strength shows the HER peak at the same potential, we assign this peak to the reduction of the protonated (DMSOH⁺). From these experiments it is evident that DMSOH⁺ is not a strong enough acid to allow for the protonation of A_4 -radical species. However, the protonation of A_4 -radical is achieved in acetonitrile (section 2D).

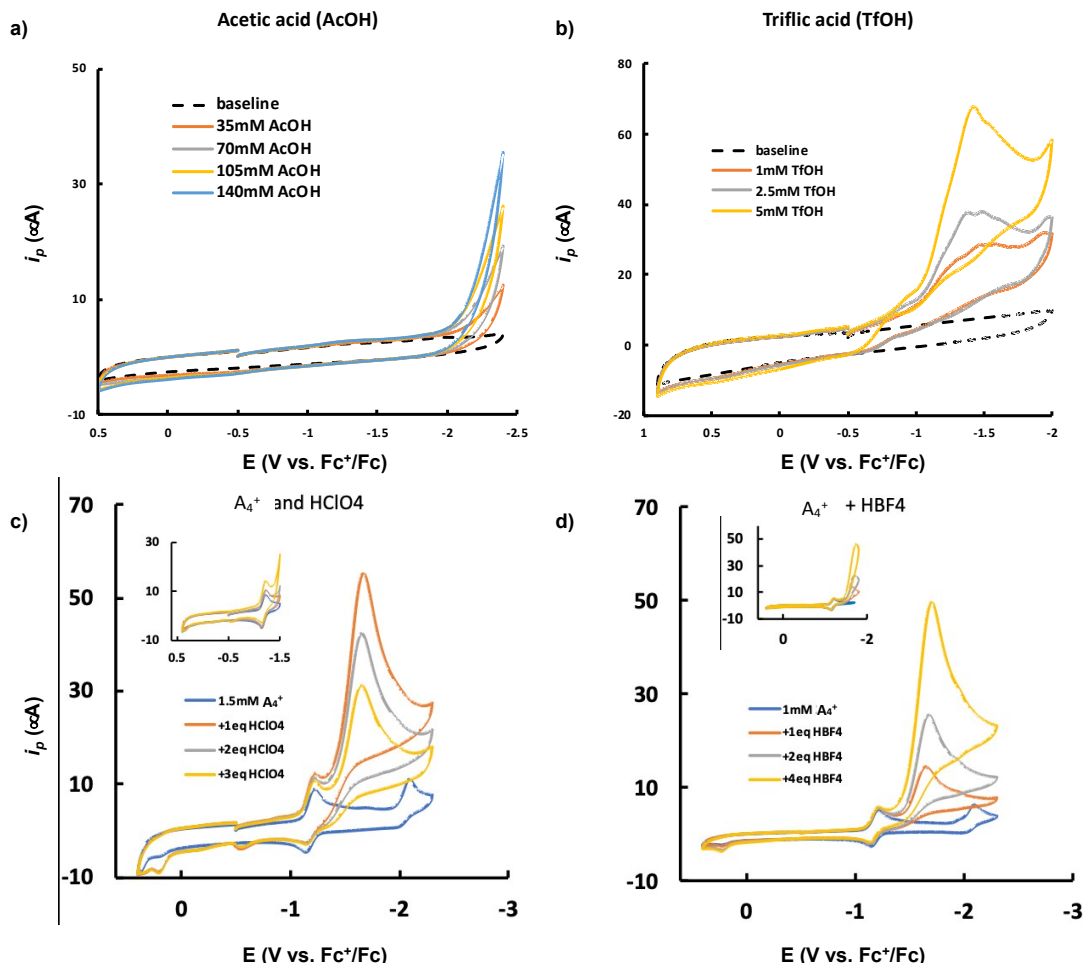


Figure S3. Cyclic voltammograms of: a) acetic acid in DMSO; b) triflic acid in MeCN, c) 2O^+ and perchloric acid in DMSO; and d) 2O^+ and tetrafluoroboronic acid in DMSO.

C. Cyclic voltammograms of authentic hydride samples

In order to confirm that the oxidation peaks in Fig 1 correspond to the formation of the hydride, we obtained cyclic voltammograms for the corresponding hydrides. For A_2H in MeCN (Fig S4b), we observe the shift of the potential to more positive values and attenuation of peak current with the addition of acid. Such behavior is consistent with the reduced rate of proton-coupled two electron oxidations of the hydride due to surpassing of the deprotonation of the forming radical cation.

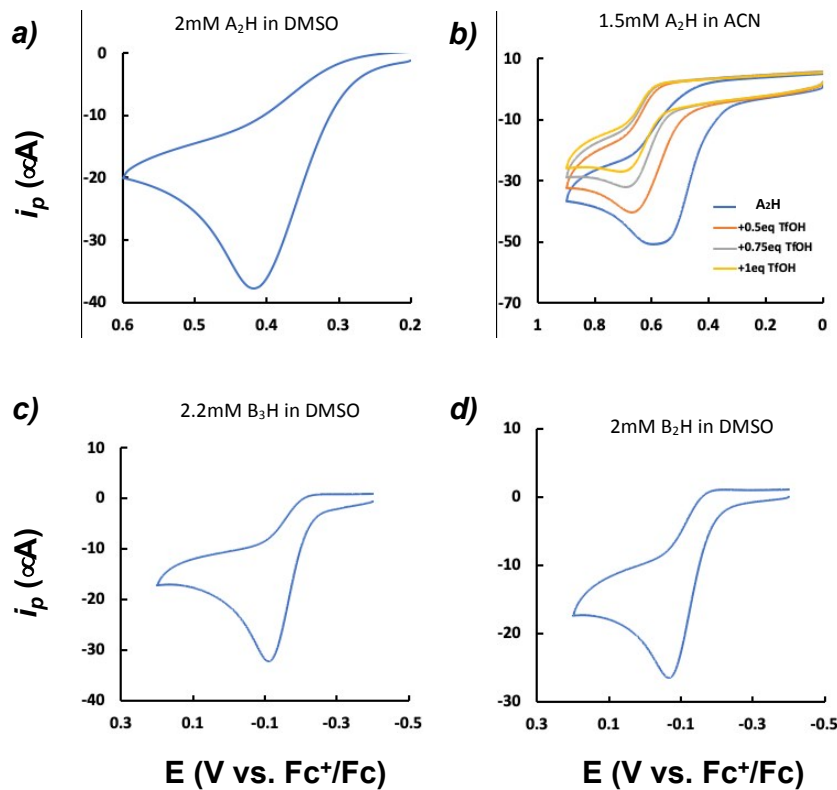


Figure S4. Cyclic voltammograms of oxidations for: a) A_2H in DMSO; b) A_2H in MeCN with addition of triflic acid; c) B_3H in DMSO; and d) B_2H in DMSO.

D. Kinetic Isotope Effect for Acridine-Hydride Regeneration with AcOH

The hydride regeneration mechanism of A_2H is studied using protic and deuterated acetic acids (Fig S5). In both cases, the addition of acid results in simultaneous increase of second reduction peak and increasing current at first reduction potential. Such behavior implies a more facile protonation of the forming anion with acetic acid than with solvent. The lack of isotope effect indicate that this conversion occurs stepwise, rather than concertedly.

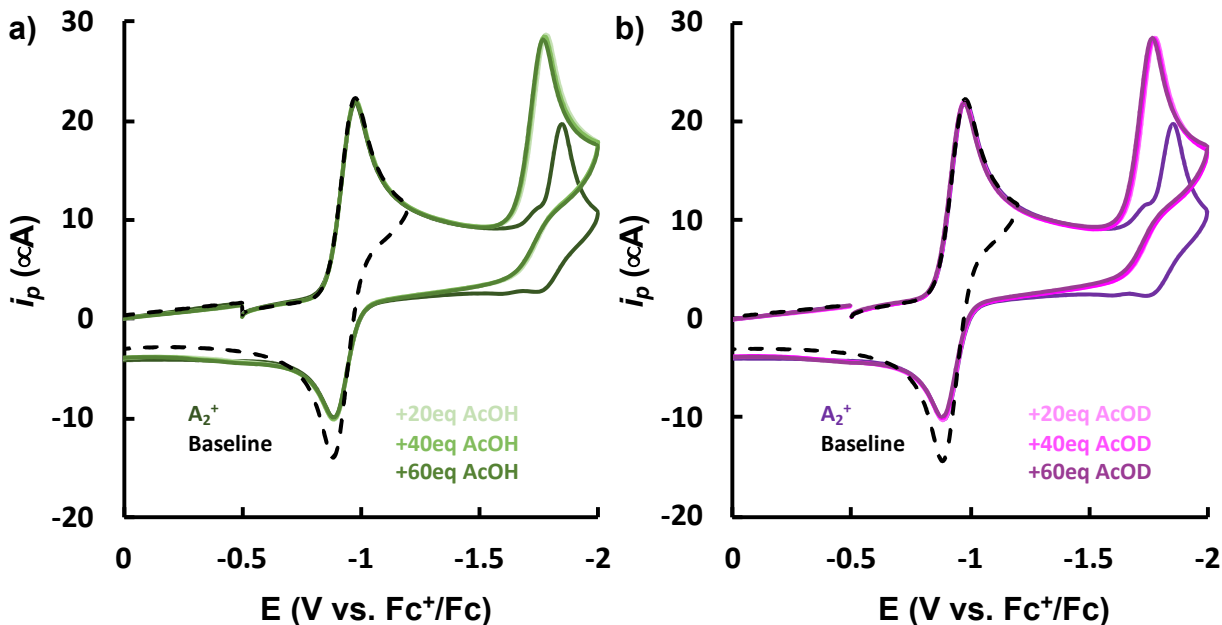


Figure S5. Cyclic voltammograms of 2.1mM A_2^+ in the presence of: a) acetic acid, AcOH; b) d-acetic acid, AcOD.

E. Protonation of A_2 -radical with HBF_4 in MeCN

As mentioned above, the protonation of poorly basic acridine-radicals cannot be achieved in DMSO, due to its higher basicity. Figure S6 shows the protonation of A_2 -radical in MeCN. The rising peak at -1.5 V vs. Fc/Fc^+ has been observed with the addition of TfOH (in main text). Similar behavior has been observed for nickel-based hydrides, and the irreversible peak between two reductions was assigned to electrocatalytic activity toward proton reduction.¹⁷

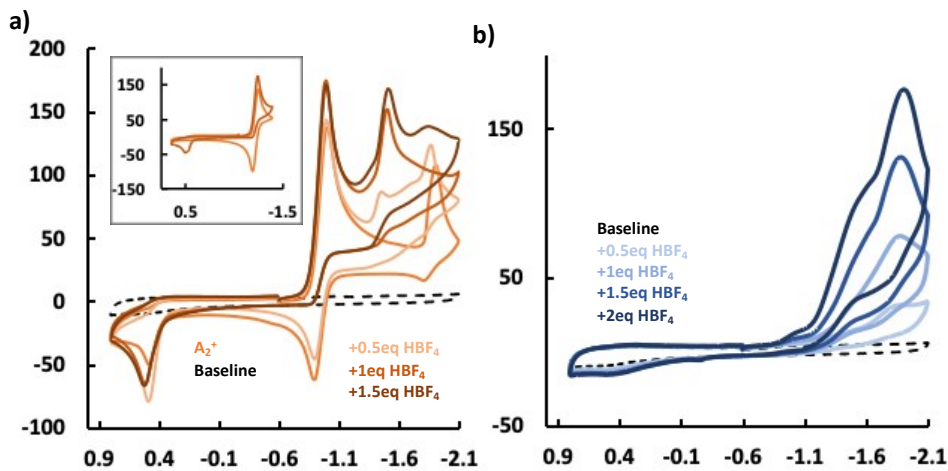


Figure S6. Cyclic voltammogram of: a) 6.4mM A_2^+ in the presence of 0.5-1.5eq of HBF_4^- ; b) 3.2-12.8mM HBF_4^- .

F. Protonation of A_4^+ -radical with TfOH in MeCN

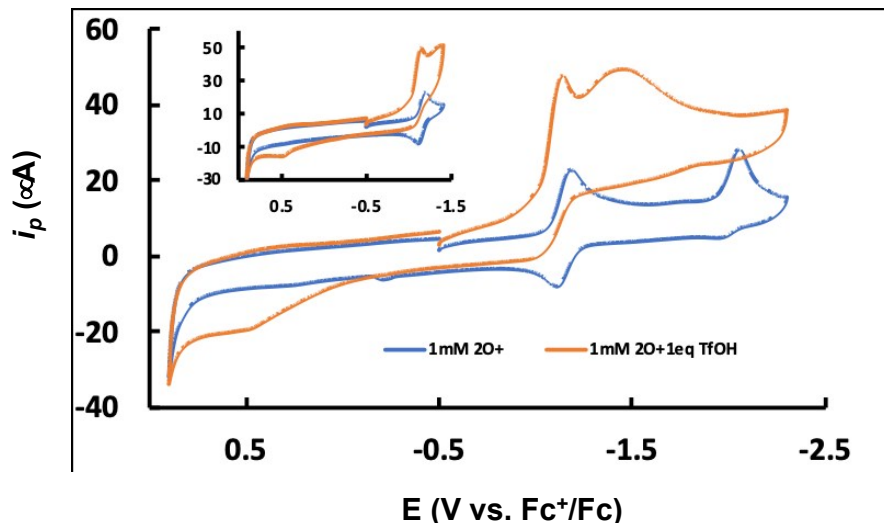


Figure S7. Cyclic voltammogram of A_4^+ in the absence (blue) and presence (orange) of strong acid (triflic acid, TfOH). Inset: conformation that triflic acid protonate the radical and consequently form a hydride.

G. UV-Vis evidence for radical protonation

Protonation of the radical was confirmed by measuring UV-Vis absorption spectra of chemically reduced radical (A_2^+) in the presence of HBF_4 -acid. First, the reduction of A_2^+ with zinc caused the color change from yellow to deep red, which was accompanied with the simultaneous disappearance of the band around 430 nm (Figure S8a A_2^+) and appearance of new band at 520 nm (Figure S8a A_2^\cdot). Then, addition of HBF_4 yielded in disappearance of the band at 520 nm and the resulting mixture displays absorption spectra (Figure S8a $\text{A}_2^\cdot + \text{HBF}_4$) with absorption features

of both A_2^+ and A_2H . Such behavior can be explained with large driving force ($\Delta G \sim 30$ kcal/mol) for the reduction of the forming protonated radical ($E^\circ(\text{A}_2\text{H}^\cdot/\text{A}_2\text{H}) = +0.28$ V vs. Fc/Fc^+) with the unreacted radical ($E^\circ(\text{A}_2^+/\text{A}_2^\cdot) = -1.07$ V vs. Fc/Fc^+):



The protonation of the radical was further validated by the deprotonation of the formed A_2H^\cdot in the presence of aqueous KOH solution ($\text{pH} = 12$). Two formed layers were separated and analyzed separately. The diethyl ether layer displayed the absorption features that are associated with A_2^\cdot and A_2H (Figure S8b $\text{A}_2^\cdot\text{-HBF}_4\text{-KOH}$), while the aqueous layer showed absorption similar to A_2^+ (not shown here). Once the organic layer was exposed to air, the color of the solution changed from deep red to yellow and showed absorbance similar to A_2^+ (Figure S8b $\text{A}_2^\cdot\text{-HBF}_4\text{-KOH-O}_2$).

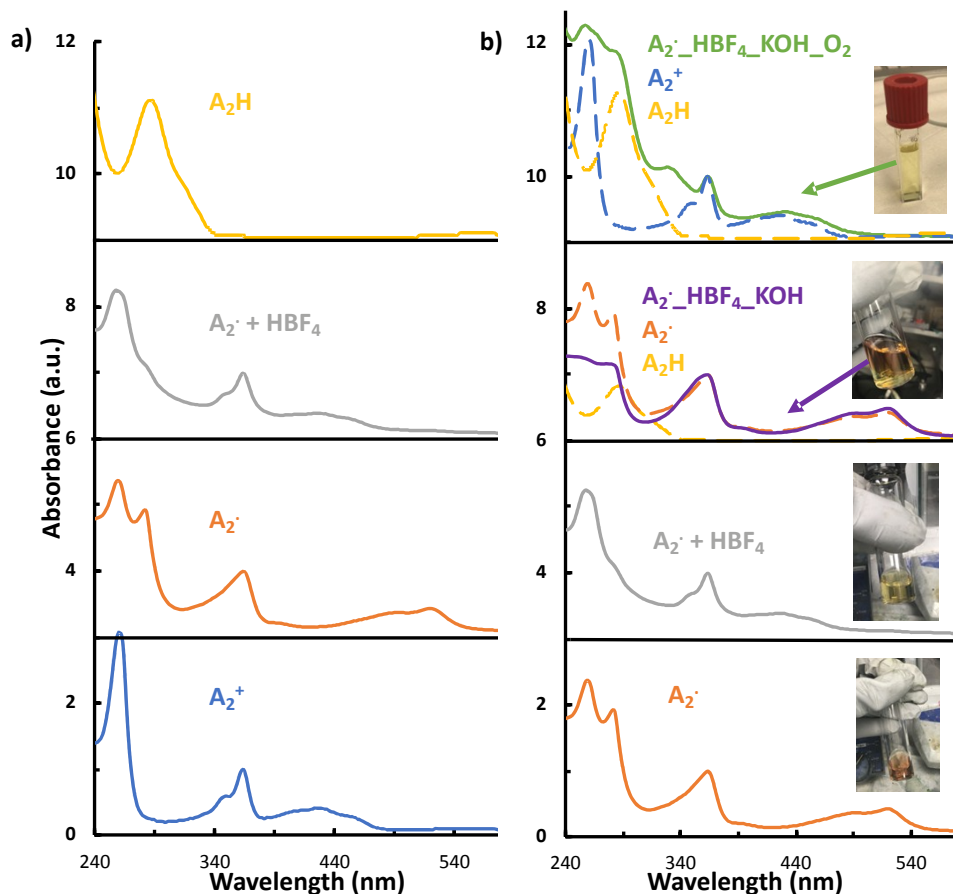


Figure S8. UV-Vis absorption experiments for radical protonation. A) Normalized spectra of A_2^+ , A_2^\cdot , $\text{A}_2\cdot\cdot$ in the presence of HBF_4 and A_2H ; b) Normalized spectra for A_2^\cdot , $\text{A}_2\cdot\cdot$ in the presence of HBF_4 , A_2^\cdot , $\text{A}_2\cdot\cdot$ / HBF_4 with addition of aqueous KOH and $\text{A}_2^\cdot\cdot$ / HBF_4 /KOH exposed to air.

H. Bulk electrolyses of acridine and benzimidazole representatives

Bulk electrolysis was performed in a glovebox using a BASi Epsilon potentiostat in a VC-2voltammetry cell (Bioanalytical Systems), with a carbon fiber paper working electrode (Freudenberg H23, Fuel Cell Store), a nonaqueous Ag/Ag^+ reference electrode (MF-2062,

Bioanalytical Systems), and a coiled platinum wire in an auxiliary electrode chamber (MW-1033 and MR1196, Bioanalytical Systems) as the counter electrode. The electrolyses were performed in deuterated DMSO-d₆ and MeCN-d₃, while the progress was monitored using ¹H NMR spectroscopy (Figure S9, S10 and S11).

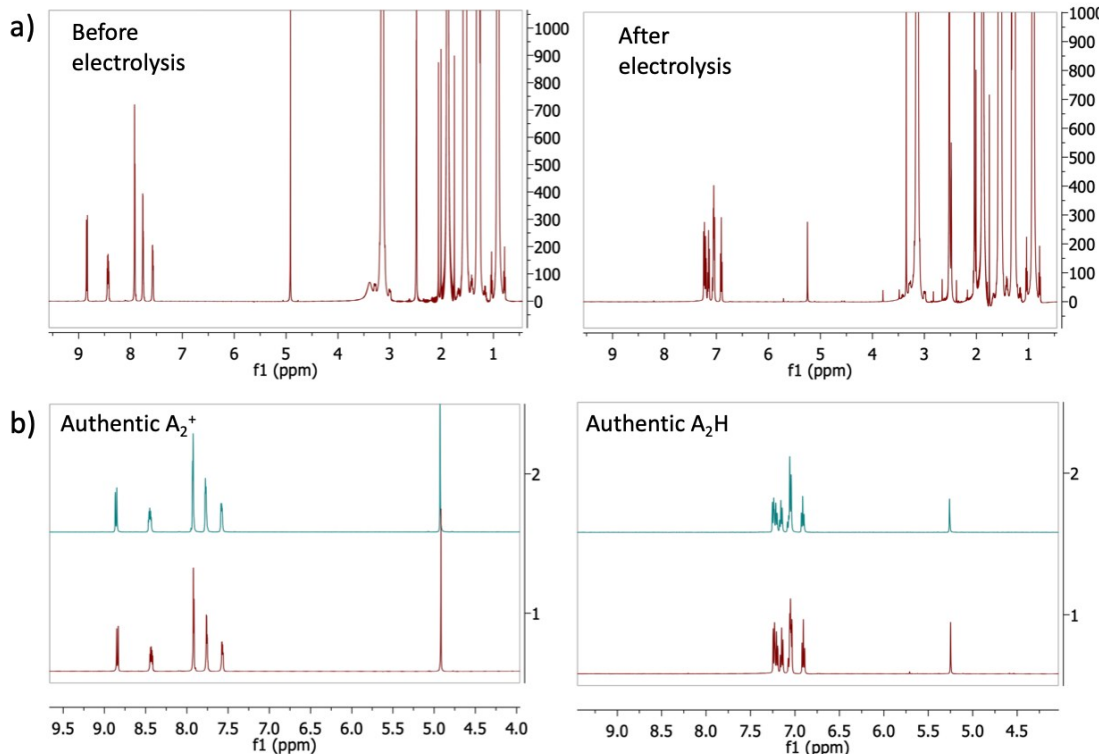


Figure S9. a) NMR spectra in DMSO-d₆ for catholyte before and after electrolysis of A_2^+ in the presence of AcOH, at applied potential of -2.0 V vs. Fc/Fc⁺. b) Comparison of catholyte solution before and after electrolysis with the authentic samples for A_2^+ and A_2H .

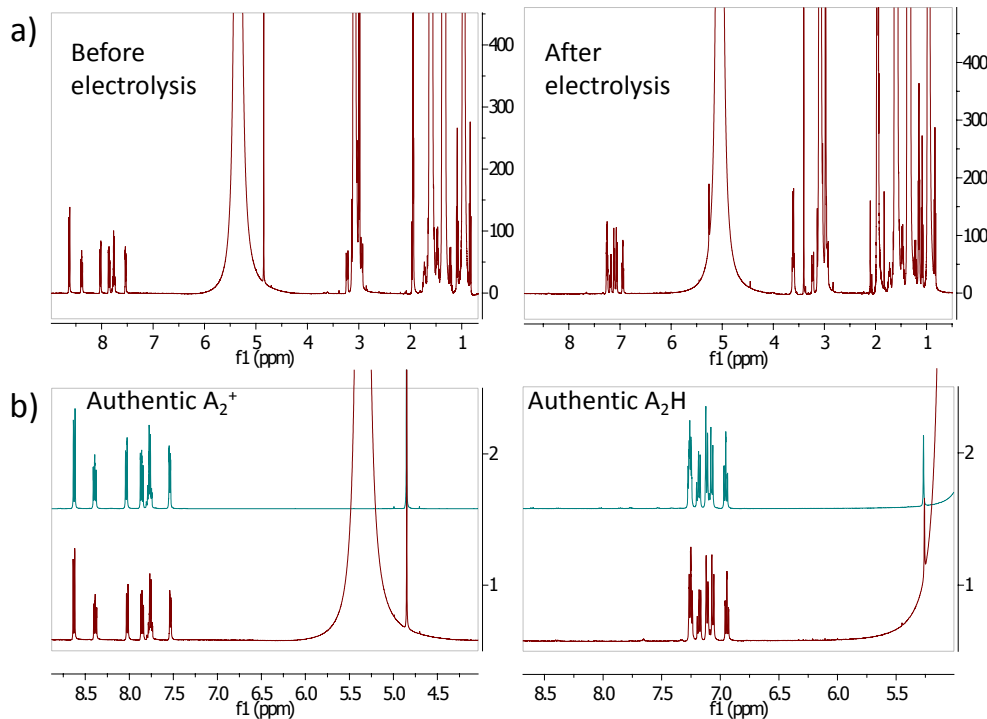


Figure S10. a) NMR spectra in MeCN-d₃ for catholyte before and after electrolysis of A₂⁺ in the presence of HBF₄, at applied potential of -1.2 V vs. Fc/Fc⁺. b) Comparison of catholyte solution before and after electrolysis with the authentic samples for A₂⁺ and A₂H.

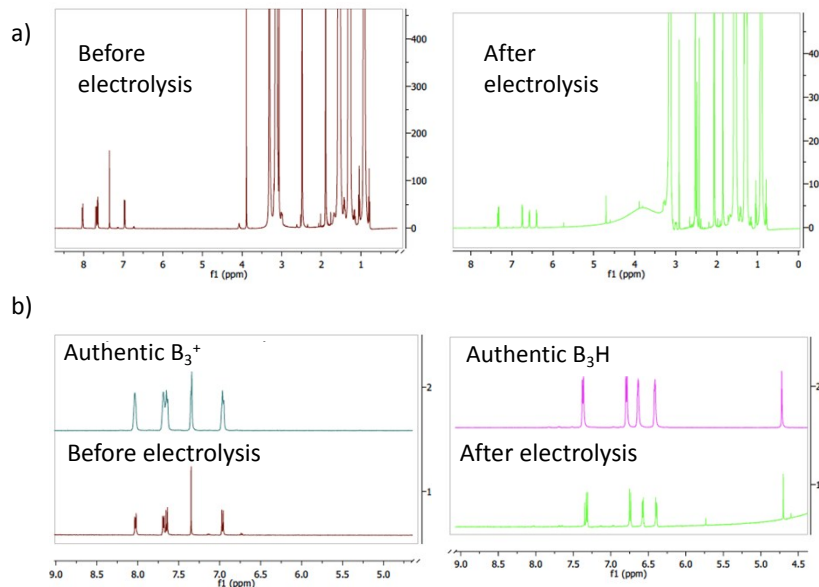


Figure S11. a) NMR spectra for catholyte before and after electrolysis of B₃⁺ in the presence of AcOH, at applied potential of -2.45 V vs. Fc/Fc⁺. b) Comparison of catholyte solution before and after electrolysis with the authentic samples for B₃⁺ and B₃H.

I. Electrochemical regeneration for some benzimidazole hydride with PhOH

Fig S12 shows the electrochemical regeneration for additional two benzimidazole hydrides using a very weak acid, such as phenol.

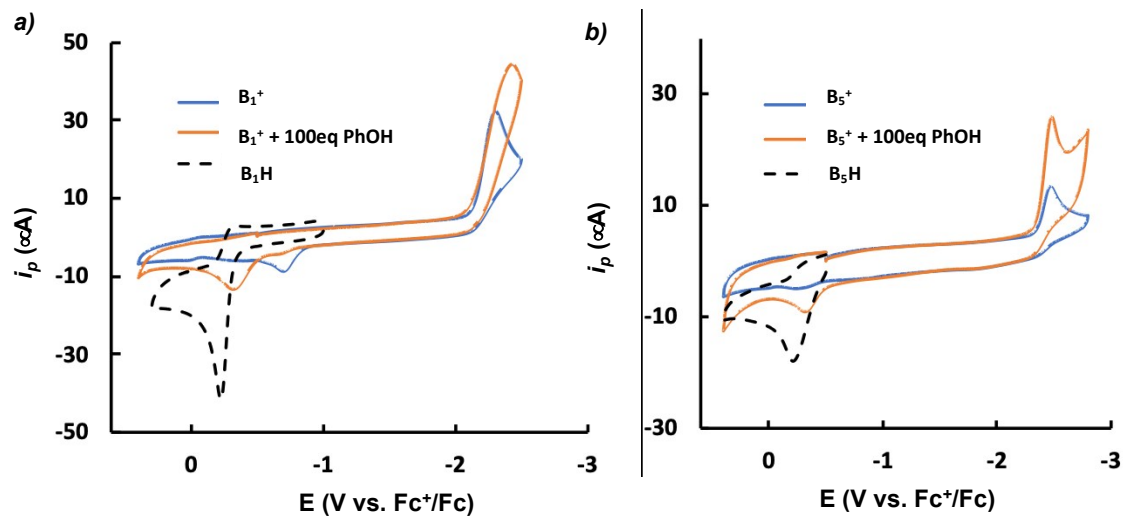


Figure S12. Electrochemical regeneration of: a) B_1^+ and b) B_5^+ with a weak proton donor.

J. Kinetic Isotope Effect for Benzimidazoles Hydride Regeneration

The mechanism of hydride regeneration of a benzimidazole representative (B_8H) is examined using protic and deuterated acetic acids (Fig S13). In both cases, the addition of acid results in simultaneous disappearance of second reduction peak and increasing current at first reduction potential. Such behavior indicates that upon addition of acid regeneration mechanism switches from EEP to EPE mechanism. The lack of isotope effect indicates that this conversion occurs in a stepwise manner rather than concertedly.

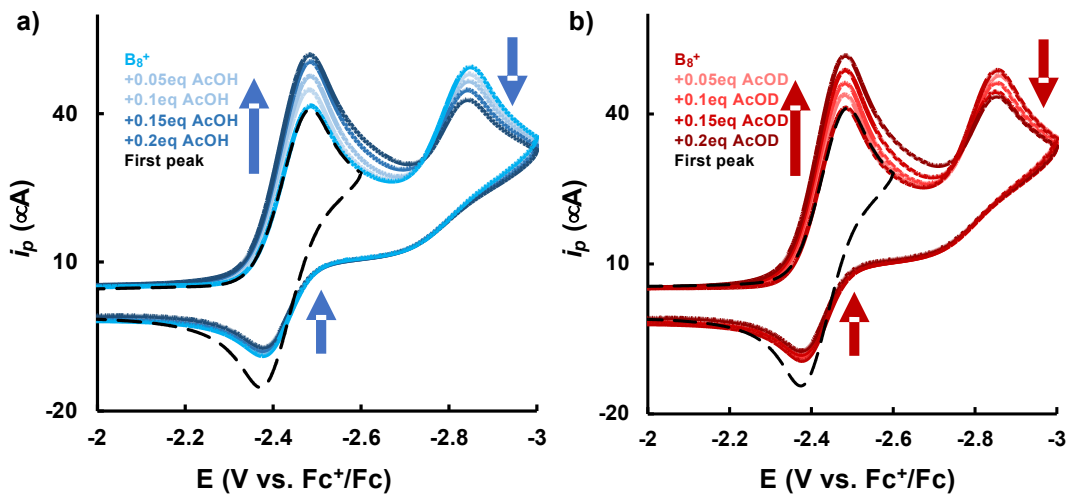


Figure S13. Cyclic voltammograms of B_8^+ in the presence of: a) acetic acid, AcOH; b) d-acetic acid, AcOD.

3) The $pK_a(RH^{+}\cdot)$ vs. $E^0_{R+/R\cdot}$ correlation

Benzimidazole derivatives display larger pKa values for $RH^{+}\cdot$ than their acridine correspondents. The improved radical protonation is a result of higher reduction potentials for the radical formation ($E^0_{R+/R\cdot}$), as shown in Fig S14.

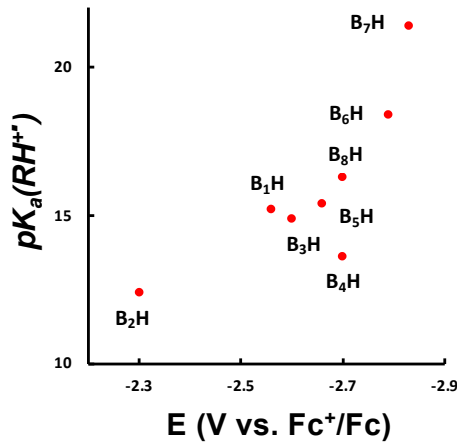


Figure S14. Acidity constant for $RH^{+}\cdot$, $pK_a(RH^{+}\cdot)$, as a function of $E^0_{R+/R\cdot}$ for benzimidazoles.

4) Molecular Coordinates

A sample of molecular coordinates is presented in this section for Radical Cations of Benzimidazole- and Acridine-based intermediates. The coordinates are expressed in the xyz-Cartesian coordinate system. Zero-point energies (ZPEs) are reported for each molecule in units of Hartree/particle. ZPEs were calculated using the wB97XD functional with 6-311G+(d,p) basis set in a CPCM-DMSO solvent.

A₄Hcat

ZPE = -1148.96

C	3.475	2.5867	-0.0625
C	2.229	3.0753	-0.3879
C	1.1057	2.2353	-0.2258
C	1.277	0.9466	0.2892
C	2.5546	0.4305	0.5067
C	3.6603	1.2663	0.3589
H	4.338	3.233	-0.1616
H	2.128	4.097	-0.7218
H	4.6625	0.9045	0.5466
C	-1.3042	1.972	-0.1175
C	-2.5739	2.5822	-0.2258
C	-3.6739	1.9308	0.2755
C	-3.5618	0.6843	0.8985
C	-2.3157	0.0842	1.0081
C	-1.177	0.7023	0.4711
H	-2.6915	3.5661	-0.6527
H	-4.647	2.4005	0.2056
H	-4.4478	0.2052	1.2916
C	0.1481	0.0338	0.6036
H	0.2553	-0.2317	1.6694
N	-0.1723	2.6521	-0.5572
C	-0.3356	3.8635	-1.3667
H	-1.193	3.7421	-2.0211
H	-0.475	4.7335	-0.7224
H	0.5427	3.9979	-1.9883
N	2.6254	-0.9268	0.8331
C	1.7354	-1.7624	0.1181
C	0.4487	-1.2692	-0.1335
C	-0.4111	-1.9858	-0.9723
C	-0.0317	-3.2429	-1.4451
C	1.2202	-3.7484	-1.1183

C	2.1207	-3.0165	-0.3604
H	-0.6983	-3.8232	-2.0681
H	1.5103	-4.7235	-1.4924
H	3.1105	-3.4084	-0.1719
C	3.8971	-1.4694	1.2815
H	3.7241	-2.4317	1.7613
H	4.6143	-1.6021	0.4627
H	4.3262	-0.7993	2.0259
O	-2.0885	-1.0984	1.606
O	-1.5873	-1.3989	-1.2855
C	-3.2	-1.8537	2.068
H	-3.7329	-1.3254	2.8634
H	-3.8846	-2.0797	1.2457
H	-2.7856	-2.7788	2.4617
C	-2.5919	-2.1678	-1.9252
H	-2.2983	-2.4398	-2.9433
H	-2.8202	-3.0715	-1.3524
H	-3.4729	-1.5294	-1.9621

A₅Hcat

ZPE = -1013.42

C	3.558	-2.061	-0.4457
C	2.3917	-2.7805	-0.3006
C	1.2105	-2.0867	0.0306
C	1.2309	-0.6996	0.2386
C	2.4177	0.0155	0.0799
C	3.5839	-0.6799	-0.2721
C	-1.2293	-0.7024	0.2386
C	-1.2058	-2.0894	0.0306
C	-2.3855	-2.7858	-0.3006
H	-2.3818	-3.8493	-0.4869
C	-3.5534	-2.0689	-0.4455
C	-3.5824	-0.6879	-0.2718
C	-2.4177	0.0101	0.0801
H	4.4692	-2.575	-0.7247
H	2.3905	-3.844	-0.4869
H	4.5131	-0.1506	-0.4314
H	-4.4634	-2.5849	-0.7244
H	-4.5128	-0.1607	-0.431
C	0	0.0082	0.7057
C	-0.0016	1.4307	0.2158

C	1.2118	2.0949	0.0326
C	-1.2165	2.0922	0.0328
C	1.2088	3.4378	-0.3567
C	-1.2165	3.435	-0.3565
C	-0.0046	4.0849	-0.5409
H	2.1319	3.973	-0.5289
H	-2.1409	3.9682	-0.5286
H	-0.0058	5.1234	-0.8514
H	0.0001	0.0071	1.8111
C	3.6623	2.1219	0.3219
H	4.3915	1.5422	0.8863
H	3.508	3.0575	0.8571
H	4.0685	2.3413	-0.6721
N	2.4061	1.3934	0.2668
C	0.0047	-4.2247	0.247
H	-0.8743	-4.5364	0.802
H	0.8843	-4.5344	0.8024
H	0.0054	-4.6856	-0.7427
N	0.0031	-2.7633	0.132
C	-3.6671	2.1136	0.3222
H	-3.5149	3.0496	0.8575
H	-4.395	1.5322	0.8866
H	-4.0738	2.3322	-0.6717
N	-2.4092	1.3879	0.2671

A₁Hcat

ZPE = -595.60

C	-12.4833	1.5667	2.4941
C	-11.1164	1.5355	2.2663
C	-10.3938	2.7097	2.1004
C	-11.076	3.9431	2.1583
C	-12.4667	3.9712	2.3912
C	-13.1549	2.7912	2.5608
C	-8.985	5.1672	2.1618
C	-8.243	3.969	2.1033
C	-6.9644	6.4164	2.5713
H	-13.0302	0.6414	2.6275
H	-10.5946	0.5869	2.2159
H	-12.9975	4.9082	2.4769
H	-14.2194	2.8186	2.7558

H	-6.4678	7.3578	2.7693
C	-8.3298	6.3936	2.3987
H	-8.8879	7.3147	2.484
C	-6.2248	5.2318	2.5035
H	-5.1504	5.2559	2.6387
C	-6.8655	4.0248	2.2718
H	-6.2931	3.1058	2.2203
N	-10.3641	5.1253	2.0073
C	-8.932	2.6801	1.8035
H	-8.803	2.462	0.7327
H	-8.4502	1.8553	2.3333
C	-11.0928	6.3704	1.7471
H	-11.3739	6.8516	2.6861
H	-10.4635	7.0342	1.1628
H	-11.9803	6.1463	1.1638

B₁Hcat

ZPE = -459.27

C	0.0001	0.7141	-0.2058
C	-0.0001	-0.7141	-0.2058
C	-0.0002	-1.4377	-1.4059
C	-0.0001	-0.709	-2.5744
C	0.0001	0.709	-2.5744
C	0.0002	1.4377	-1.4059
C	0	0	1.9688
H	-0.0004	-2.5197	-1.408
H	-0.0002	-1.2293	-3.5242
H	0.0002	1.2293	-3.5242
H	0.0004	2.5197	-1.408
H	-0.8929	0	2.6058
H	0.8929	0	2.6058
N	0	1.1323	1.0687
N	0	-1.1323	1.0687
C	0.0005	2.5094	1.5214
H	0.8939	3.0226	1.1611
H	-0.8905	3.0242	1.1574
H	-0.0018	2.522	2.6093
C	-0.0005	-2.5094	1.5214
H	-0.8939	-3.0226	1.1611
H	0.8905	-3.0242	1.1574
H	0.0018	-2.522	2.6093

B₆Hcat

ZPE = -655.71

C	0.3034	-0.7172	-0.0666
C	0.3109	0.7174	-0.0679
C	-0.8812	1.4614	0.0486
C	-2.0629	0.7344	0.0027
C	-2.069	-0.7043	-0.0142
C	-0.8978	-1.4451	0.0376
C	2.4919	-0.0133	-0.2197
H	3.0448	-0.0201	-1.1687
N	1.5794	-1.1396	-0.1918
N	1.5922	1.1238	-0.2004
C	2.0963	-2.4778	-0.419
H	2.2527	-3.0113	0.5207
H	1.4167	-3.0398	-1.0555
H	3.0529	-2.3906	-0.934
C	2.1264	2.4505	-0.4559
H	1.4477	3.0124	-1.0935
H	2.3032	2.9972	0.4725
H	3.075	2.3397	-0.9809
C	3.4672	-0.0138	0.9546
H	4.1013	-0.9005	0.9093
H	4.1105	0.8658	0.9022
H	2.9163	-0.0071	1.8967
C	-0.9129	-2.9411	0.2339
H	-0.9962	-3.483	-0.7131
H	-0.0144	-3.2848	0.7423
H	-1.756	-3.2342	0.8584
C	-3.3972	-1.4161	-0.0237
H	-3.3086	-2.4348	-0.3961
H	-3.8234	-1.4621	0.9848
H	-4.1198	-0.8995	-0.6547
C	-3.3952	1.437	-0.0016
H	-3.9281	1.2285	-0.934
H	-4.0312	1.0887	0.8165
H	-3.3011	2.5162	0.0773
C	-0.8586	2.9574	0.2499
H	0.0675	3.282	0.7185
H	-0.9745	3.504	-0.6905
H	-1.6632	3.2676	0.9151

B₅Hcat

ZPE = -498.57

C	-0.4904	-0.7148	-0.087
C	-0.4904	0.7148	-0.087
C	-1.6857	1.4361	0.0495
C	-2.8468	0.7091	0.178
C	-2.8467	-0.7093	0.178
C	-1.6856	-1.4362	0.0495
C	1.6889	0.0001	-0.2875
H	-1.6911	2.5177	0.0586
H	-3.7898	1.2304	0.2868
H	-3.7897	-1.2306	0.2868
H	-1.691	-2.5178	0.0586
H	2.2126	0.0001	-1.2526
N	0.7747	-1.1318	-0.2368
N	0.7747	1.1318	-0.2368
C	1.2399	-2.5036	-0.2528
H	1.4512	-2.8526	0.7608
H	0.4793	-3.139	-0.7042
H	2.1466	-2.5649	-0.8535
C	1.2396	2.5037	-0.2528
H	0.4794	3.1388	-0.7052
H	1.4498	2.8531	0.7609
H	2.1469	2.5649	-0.8526
C	2.6955	0.0001	0.8583
H	3.3326	-0.8824	0.7878
H	3.3324	0.8826	0.7879
H	2.1757	0	1.8178

B₄Hcat

ZPE = -808.09

C	-2.2484	0.2316	-0.6952
C	-2.2546	0.029	0.7193
C	-3.397	-0.4522	1.3747
C	-4.4998	-0.7212	0.5972
C	-4.4939	-0.5197	-0.8069
C	-3.3851	-0.0446	-1.4686
C	-0.1983	0.8821	0.1292

H	-3.409	-0.5985	2.4464
H	-5.4024	-1.0923	1.0667
H	-5.3922	-0.7426	-1.3691
H	-3.3885	0.1161	-2.5384
H	-0.1234	1.9659	0.2835
N	-1.0311	0.6663	-1.051
N	-1.0417	0.3466	1.1937
C	-0.6037	1.051	-2.3796
H	-1.0711	0.3955	-3.1135
H	-0.8755	2.0888	-2.5869
H	0.478	0.937	-2.446
C	-0.625	0.3409	2.58
H	-0.8801	1.2868	3.0638
H	-1.1146	-0.481	3.1009
H	0.4537	0.1904	2.621
C	1.1949	0.2913	0.0499
C	1.3893	-1.0913	-0.1296
C	2.2961	1.1561	0.1601
C	2.6912	-1.5764	-0.1992
C	3.5807	0.6207	0.0841
C	3.7998	-0.7395	-0.0986
H	2.8442	-2.6427	-0.3353
H	4.4322	1.2883	0.1716
C	5.1943	-1.2936	-0.211
H	5.4812	-1.3892	-1.2628
H	5.9217	-0.64	0.2736
H	5.2627	-2.2859	0.2396
C	0.2514	-2.0755	-0.242
H	-0.3506	-2.103	0.6694
H	-0.4153	-1.8357	-1.0731
H	0.64	-3.08	-0.4103
C	2.1501	2.6465	0.3619
H	1.6168	3.1225	-0.4656
H	1.6156	2.8843	1.2857
H	3.1335	3.1127	0.4256

B₇Hcat

ZPE = -632.47

C	-0.3847	0.4754	-0.1646
C	-0.7817	-0.9005	-0.1406
C	0.1813	-1.9096	-0.0404

C	1.5036	-1.5424	0.0279
C	1.9119	-0.1661	0.0065
C	0.9397	0.8516	-0.0855
C	-2.6957	0.3863	-0.2249
H	-0.1006	-2.954	-0.0116
H	2.2475	-2.3216	0.1055
H	1.2084	1.8968	-0.0869
H	-3.2944	0.5287	-1.1338
N	-1.5025	1.2196	-0.2802
N	-2.1195	-0.9554	-0.233
C	-1.5591	2.6634	-0.2865
H	-1.5091	3.0728	0.7269
H	-0.728	3.0574	-0.8734
H	-2.4892	2.9837	-0.7559
C	-2.9372	-2.1479	-0.1974
H	-2.4063	-2.9666	-0.6822
H	-3.1767	-2.4306	0.8312
H	-3.8618	-1.9625	-0.7439
C	-3.5494	0.646	1.0114
H	-3.9214	1.6717	0.9944
H	-4.4111	-0.0237	1.0199
H	-2.9591	0.4904	1.9169
N	3.2329	0.1403	0.0798
C	4.2477	-0.9001	0.1967
H	4.2433	-1.56	-0.6749
H	5.2252	-0.4294	0.2597
H	4.1007	-1.4984	1.0996
C	3.6556	1.5323	0.0502
H	3.254	2.0846	0.9053
H	4.7405	1.5768	0.0926
H	3.3275	2.0221	-0.8714

A₃Hcat

ZPE = -960.44

C	-12.4814	1.5923	2.5749
C	-11.094	1.5669	2.479
C	-10.3706	2.7134	2.1725
C	-11.0531	3.9214	1.9567
C	-12.4474	3.9485	2.0651
C	-13.1519	2.7892	2.3654
C	-9.0348	5.1954	2.1904

C	-8.2741	4.0367	2.415
C	-7.2152	6.5372	3.052
H	-13.0271	0.6857	2.8071
H	-10.5717	0.6286	2.6293
H	-12.9901	4.8746	1.9298
H	-14.2325	2.832	2.4435
H	-6.8163	7.5141	3.3013
C	-8.4963	6.4428	2.5226
H	-9.0766	7.3451	2.3833
C	-6.4582	5.3948	3.271
H	-5.4581	5.4641	3.6815
C	-6.9976	4.153	2.9524
H	-6.4007	3.2617	3.1112
N	-10.3158	5.0694	1.6363
C	-8.8635	2.7091	1.9613
H	-8.6916	2.6359	0.8784
C	-11.0155	6.2601	1.1921
H	-11.4677	6.8254	2.0169
H	-10.3185	6.908	0.6616
H	-11.7979	5.9752	0.4895
C	-8.1933	1.5281	2.6141
C	-8.2495	1.3622	4.0132
C	-7.5049	0.5775	1.8493
C	-7.6516	0.2976	4.6273
H	-8.7725	2.0976	4.613
C	-6.8841	-0.4965	2.4383
H	-7.4641	0.6869	0.7721
C	-6.9411	-0.6685	3.852
H	-7.6957	0.2123	5.7034
H	-6.3797	-1.2224	1.8168
N	-6.339	-1.7167	4.4418
C	-5.4589	-2.6165	3.6989
H	-4.8298	-3.1453	4.4096
H	-6.0564	-3.3422	3.1413
H	-4.824	-2.0544	3.0178
C	-6.5322	-2.0155	5.8593
H	-6.2562	-3.0521	6.0325
H	-5.8921	-1.3689	6.4649
H	-7.5738	-1.8771	6.1404

B₃Hcat
ZPE = -824.12

C	2.7387	0.7112	-0.004
C	2.733	-0.7189	-0.0353
C	3.7808	-1.4566	0.5358
C	4.7999	-0.7464	1.1266
C	4.8053	0.6723	1.1579
C	3.7917	1.4155	0.5989
C	0.8436	0.028	-1.1315
H	3.7868	-2.5379	0.5055
H	5.6273	-1.2805	1.5771
H	5.6366	1.1798	1.6313
H	3.8057	2.497	0.6158
H	0.8793	0.051	-2.2306
N	1.6261	1.1469	-0.6089
N	1.6168	-1.119	-0.6577
C	1.2564	2.5242	-0.8572
H	1.598	3.1469	-0.0315
H	1.6982	2.8779	-1.7919
H	0.1704	2.5884	-0.9202
C	1.2373	-2.4806	-0.9692
H	1.6748	-2.7932	-1.9205
H	1.5763	-3.1436	-0.1743
H	0.1508	-2.5346	-1.0325
C	-0.5891	0.0247	-0.6727
C	-0.8999	-0.0022	0.6873
C	-1.6314	0.0453	-1.5925
C	-2.2108	-0.0045	1.1194
H	-0.1032	-0.0236	1.4252
C	-2.9537	0.0431	-1.1793
H	-1.4132	0.0616	-2.6559
C	-3.2819	0.025	0.1935
H	-2.4069	-0.0292	2.1825
H	-3.7317	0.0554	-1.93
N	-4.5819	0.0377	0.6156
C	-5.6585	-0.0233	-0.3547
H	-5.6236	-0.9449	-0.9486
H	-6.6119	0.0072	0.1688
H	-5.6263	0.8299	-1.04
C	-4.8892	-0.0804	2.0287
H	-4.4556	0.7452	2.6022
H	-5.9684	-0.0458	2.1618
H	-4.5233	-1.0244	2.4508

B₈Hcat

ZPE = -1033.70

C	2.6374	0.3787	0.7151
C	2.6374	0.3792	-0.7149
C	3.7531	-0.0707	-1.4358
C	4.8391	-0.5026	-0.7092
C	4.839	-0.5031	0.709
C	3.7529	-0.0717	1.4357
C	0.5776	1.1247	0.0003
H	3.7542	-0.0835	-2.5175
H	5.7193	-0.8577	-1.2308
H	5.7192	-0.8587	1.2303
H	3.7539	-0.0854	2.5175
H	0.3424	2.1953	0.0006
N	1.4513	0.8355	1.1336
N	1.4513	0.8362	-1.1332
C	0.9658	0.8753	2.4956
H	0.5347	-0.0898	2.7752
H	1.7869	1.1188	3.1684
H	0.2017	1.6475	2.5782
C	0.966	0.8773	-2.4951
H	1.7872	1.1214	-3.1676
H	0.5349	-0.0874	-2.7756
H	0.2021	1.6497	-2.5771
C	-0.7178	0.3585	0
C	-0.7341	-1.0472	-0.0003
C	-1.9381	1.0416	0.0001
C	-1.9275	-1.7509	-0.0005
C	-3.1523	0.3523	0
C	-3.1303	-1.0401	-0.0003
H	-1.9627	-2.8308	-0.0006
H	-4.0861	0.8915	-0.0001
O	-1.8629	2.3889	0.0004
O	-4.2438	-1.7999	-0.0004
O	0.4802	-1.6312	-0.0005
C	0.567	-3.0493	-0.0004
H	0.1012	-3.4693	0.8951
H	0.1014	-3.4695	-0.8959
H	1.6304	-3.278	-0.0002
C	-5.5121	-1.1584	-0.0002
H	-5.6423	-0.5438	-0.8953

H	-6.2485	-1.9588	-0.0002
H	-5.6421	-0.5441	0.8953
C	-3.0622	3.1522	0.0007
H	-3.6553	2.9497	0.8965
H	-2.7476	4.1932	0.001
H	-3.6554	2.9503	-0.8952

A₂Hcat

ZPE = -826.54

C	-12.5137	1.5941	2.5111
C	-11.1414	1.5492	2.3174
C	-10.4002	2.7127	2.1556
C	-11.0781	3.95	2.1696
C	-12.4732	3.9924	2.3752
C	-13.1768	2.8228	2.5496
C	-8.9905	5.1731	2.1734
C	-8.2424	3.9771	2.1597
C	-6.9825	6.4526	2.5616
H	-13.0694	0.6734	2.6399
H	-10.6318	0.5939	2.295
H	-12.9959	4.9359	2.4343
H	-14.2447	2.8627	2.7228
H	-6.4958	7.4034	2.7376
C	-8.3463	6.4107	2.383
H	-8.9136	7.328	2.4411
C	-6.2345	5.2735	2.5234
H	-5.1601	5.3081	2.6553
C	-6.8656	4.0548	2.3258
H	-6.2812	3.1432	2.3038
N	-10.3655	5.1273	2.0006
C	-8.9186	2.6585	1.8832
H	-8.8226	2.4985	0.7978
C	-11.089	6.3641	1.6875
H	-11.3837	6.8769	2.6053
H	-10.4498	7.0069	1.0908
H	-11.9673	6.1214	1.0981
C	-8.2367	1.4913	2.5755
C	-8.2005	1.4317	3.9696
C	-7.6453	0.4744	1.8343
C	-7.5801	0.3687	4.6099
H	-8.6602	2.2215	4.5556

C	-7.022	-0.5938	2.4757
H	-7.6698	0.5133	0.7502
C	-6.9884	-0.648	3.8628
H	-7.5569	0.3312	5.693
H	-6.5641	-1.3809	1.8877
H	-6.5038	-1.4783	4.3636

B₂Hcat

ZPE = -690.22

C	-1.6923	-0.715	-0.1316
C	-1.6923	0.7151	-0.1315
C	-2.8188	1.437	0.289
C	-3.9102	0.7097	0.7032
C	-3.9103	-0.7095	0.7032
C	-2.8189	-1.4369	0.2888
C	0.3424	0	-0.9419
H	-2.8276	2.5186	0.281
H	-4.8	1.2305	1.0347
H	-4.8001	-1.2303	1.0346
H	-2.8278	-2.5184	0.2809
H	0.493	0	-2.0307
N	-0.4976	-1.1333	-0.5727
N	-0.4975	1.1333	-0.5726
C	-0.0901	-2.503	-0.8095
H	-0.5458	-3.1514	-0.0626
H	-0.3907	-2.8241	-1.8097
H	0.9935	-2.5695	-0.7162
C	-0.0899	2.503	-0.8091
H	-0.3908	2.8245	-1.809
H	-0.5452	3.1512	-0.0618
H	0.9937	2.5693	-0.7162
C	1.685	-0.0001	-0.242
C	1.7407	-0.0004	1.1513
C	2.8565	0.0003	-0.989
C	2.9705	-0.0004	1.7921
H	0.8247	-0.0007	1.7331
C	4.0903	0.0003	-0.3439
H	2.8089	0.0005	-2.0728
C	4.1466	0	1.0438
H	3.015	-0.0007	2.8748
H	5.0033	0.0006	-0.9274

H 5.1067 0 1.5468

A₆Hcat

ZPE = -595.60

C	-14.8189	-0.7167	2.285
C	-13.4361	-0.7039	2.2839
C	-12.7459	0.5072	2.2853
C	-13.4412	1.7207	2.2879
C	-14.8473	1.6897	2.289
C	-15.5254	0.488	2.2876
C	-12.6816	2.9662	2.2892
C	-11.2419	2.928	2.2878
C	-10.5013	4.1471	2.2891
H	-9.4217	4.1243	2.288
C	-11.1513	5.3473	2.2917
C	-12.5587	5.3894	2.2932
C	-13.2946	4.2209	2.292
H	-15.3514	-1.6602	2.2839
H	-12.8817	-1.6361	2.2819
H	-15.4197	2.6074	2.291
H	-16.6085	0.4825	2.2884
H	-10.5816	6.2678	2.2927
H	-13.0686	6.3446	2.2953
H	-14.3728	4.2916	2.2932
N	-10.589	1.7561	2.2852
C	-11.255	0.4676	2.2839
H	-10.8933	-0.0831	3.1606
H	-10.8949	-0.0805	1.4049
C	-9.1275	1.6889	2.2836
H	-8.7308	2.1716	1.3898
H	-8.729	2.1687	3.1781
H	-8.8313	0.6436	2.2816

5) References

1. (a) J.-D. Chai and M. Head-Gordon, *Phys. Chem. Chem. Phys.*, 2008, **10**, 6615-6620; (b) M. J. Frisch, G. W. Trucks, H. B. Schlegel, G. E. Scuseria, M. A. Robb, J. R. Cheeseman, G. Scalmani, V. Barone, G. A. Petersson, H. Nakatsuji, X. Li, M. Caricato, A. V. Marenich, J. Bloino, B. G. Janesko, R. Gomperts, B. Mennucci, H. P. Hratchian, J. V. Ortiz, A. F. Izmaylov, J. L. Sonnenberg, Williams, F. Ding, F. Lipparini, F. Egidi, J. Goings, B. Peng, A. Petrone, T. Henderson, D. Ranasinghe, V. G. Zakrzewski, J. Gao, N. Rega, G. Zheng, W. Liang, M. Hada, M. Ehara, K. Toyota, R. Fukuda, J. Hasegawa, M. Ishida, T. Nakajima, Y. Honda, O. Kitao, H. Nakai, T. Vreven, K. Throssell, J. A. Montgomery Jr., J. E. Peralta, F. Ogliaro, M. J. Bearpark, J. J. Heyd, E. N. Brothers, K. N. Kudin, V. N. Staroverov, T. A. Keith, R. Kobayashi, J. Normand, K. Raghavachari, A. P. Rendell, J. C. Burant, S. S. Iyengar, J. Tomasi, M. Cossi, J. M. Millam, M. Klene, C. Adamo, R. Cammi, J. W. Ochterski, R. L. Martin, K. Morokuma, O. Farkas, J. B. Foresman and D. J. Fox, *Journal*, 2016.
2. P. C. Hariharan and J. A. Pople, *Theor Chim Acta*, 1973, **28**, 213-222.
3. (a) H. Li, C. S. Pomelli and J. H. Jensen, *Theor Chim Acta*, 2003, **109**, 71-84; (b) H. Li and J. H. Jensen, *J. Comput. Chem.*, 2004, **25**, 1449-1462.
4. S. Ilic, U. Pandey Kadel, Y. Basdogan, J. A. Keith and K. D. Glusac, *J. Am. Chem. Soc.*, 2018, **140**, 4569-4579.
5. M. Namazian, C. Y. Lin and M. L. Coote, *J. Chem. Theory Comput.*, 2010, **6**, 2721-2725.
6. B. Thapa and H. B. Schlegel, *J. Phys. Chem. A*, 2016, **120**, 5726-5735.
7. F. G. Bordwell, *Acc. Chem. Res.*, 1988, **21**, 456-463.
8. G. Wang, W. Hu, Z. Hu, Y. Zhang, W. Yao, L. Li, Z. Fu and W. Huang, *Green Chemistry*, 2018.
9. S. Ilic, E. S. Brown, Y. Xie, S. Maldonado and K. D. Glusac, *J. Phys. Chem. C*, 2016, **120**, 3145-3155.
10. X.-Q. Zhu, M.-T. Zhang, A. Yu, C.-H. Wang and J.-P. Cheng, *J. Am. Chem. Soc.*, 2008, **130**, 2501-2516.
11. A. G. Wright, T. Weissbach and S. Holdcroft, *Angew. Chem.*, 2016, **55**, 4818-4821.
12. C.-H. Lim, S. Ilic, A. Alherz, B. T. Worrell, S. S. Bacon, J. T. Hynes, K. D. Glusac and C. B. Musgrave, *J. Am. Chem. Soc.*, 2018, **Vol.**
13. Z. Bin, Z. Liu and L. Duan, *J. Phys. Chem. Lett.*, 2017, **8**, 4769-4773.
14. I.-S. H. Lee, E. H. Jeoung and M. M. Kreevoy, *Journal of the American Chemical Society*, 1997, **119**, 2722-2728.
15. V. V. Pavlishchuk and A. W. Addison, *Inorganica Chim. Acta*, 2000, **298**, 97-102.
16. B. D. McCarthy, D. J. Martin, E. S. Rountree, A. C. Ullman and J. L. Dempsey, *Inorg. Chem.*, 2014, **53**, 8350-8361.
17. D. K. Bediako, B. H. Solis, D. K. Dogutan, M. M. Roubelakis, A. G. Maher, C. H. Lee, M. B. Chambers, S. Hammes-Schiffer and D. G. Nocera, *Proc. Natl. Acad. Sci. U.S.A.*, 2014, **111**, 15001-15006.